International Journal of Mechanical and Materials Engineering (IJMME), Vol. 4 (2009), No. 3, 256-265

EFFECT OF A HEAT CONDUCTING HORIZONTAL CIRCULAR CYLINDER ON MHD MIXED CONVECTION IN A LID-DRIVEN CAVITY ALONG WITH JOULE HEATING

M. M. Rahman[1], M. A. H. Mamun[2], R. Saidur[3] and Shuichi Nagata[2]

[1]Department of Mathematics
Bangladesh University of Engineering and Technology (BUET), Dhaka-1000, Bangladesh
[2]The Institute of Ocean Energy, Saga University, Japan
[3]Department of Mechanical Engineering,
University of Malaya, 50603 Kuala Lumpur, Malaysia
Email: mmustafizurrahman@math.buet.ac.bd

ABSTRACT

Magnetohydrodynamic (MHD) mixed convection in a lid-driven cavity along with joule heating is studied numerically. The cavity consists of adiabatic horizontal walls and differentially heated vertical walls, but it also contains a heat conducting horizontal circular cylinder located somewhere within the cavity. The aim of the study is to delineate the effect of such a cylinder on the flow and temperature fields. The governing equations are first transformed into a non-dimensional form and resulting nonlinear system of partial differential equations are then solved by using Galerkin weighted residual method of finite element formulation. The analysis is conducted by observing variations of the streamlines and isotherms for the size, locations and thermal conductivity of the cylinder at the Richardson number *Ri* ranging from 0.0 to 5.0, Prandtl number *Pr* = 0.71 and Reynolds number *Re* = 100 with constant physical properties. The results indicated that both the streamlines and isotherms strongly depend on the size and locations of the inner cylinder, but the thermal conductivity of the cylinder has significant effect only on the isothermal lines. The variations of average Nusselt number on the hot wall and average fluid temperature in the cavity are also presented to show the overall heat transfer characteristics inside the cavity.

Keywords: Mixed convection, Finite element method, circular cylinder, lid-driven cavity, joule heating and Magnetohydrodynamic

NOMENCLUTURE

B_0	magnetic induction (Wb/m^2)
C_p	Specific heat of fluid at constant pressure
d	dimensional cylinder diameter (m)
D	non dimensional cylinder diameter
g	gravitational acceleration (ms^{-2})
Gr	Grashof number
h	convective heat transfer coefficient(Wm^{-2}K^{-1})
Ha	Hartmann number
J	Joule heating parameter
k_f	thermal conductivity of the fluid (Wm^{-1}K^{-1})
k_s	thermal conductivity of the solid (Wm^{-1}K^{-1})
K	solid fluid thermal conductivity ratio
l_x	dimensional distance between y-axis and the cylinder center (m)
l_y	dimensional distance between x-axis and the cylinder center (m)
L_x	dimensionless distance between y-axis and the cylinder center
L_y	dimensionless distance between x-axis and the cylinder center
L	length of the cavity (m)
Nu	average Nusselt number
p	dimensional pressure (Nm^{-2})
P	dimensionless pressure
Pr	Prandtl number
Re	Reynolds number
Ri	Richardson number
Ra	Raleigh number
T	dimensional temperature (K)
ΔT	temperature difference (K)
u, v	dimensional velocity components (ms^{-1})
U, V	dimensionless velocity components
U_0	lid velocity
$\overline{V}$	cavity volume (m^3)
x, y	Cartesian coordinates (m)
X, Y	dimensionless cartesian coordinates

Greek symbols

α	thermal diffusivity (m^{2}s^{-1})
β	thermal expansion coefficient (K^{-1})
ν	kinematic viscosity (m^{2}s^{-1})
θ	dimensionless temperature
μ	dynamic viscosity (m^{2}s^{-1})
ρ	density of the fluid (kgm^{-3})
σ	fluid electrical conductivity (Ω^{-1}.m^{-1})
ψ	stream function

Subscripts

av	average
h	heated wall
c	cold wall
s	solid

1. INTRODUCTION

1.1 Literature Review

Mixed convection phenomenon occur in many engineering systems such as cooling of electronic devices, drying technology, solar collectors, flat glass manufacturing and nuclear reactors etc. The cavity with moving lid is the most important application for these heat transfer mechanism, which is seen in cooling of electronic chips, solar energy collection and food industry etc (Jaluria & Torrance, 1986). Numerical analysis of these kinds of systems can be found in many literatures. Moallemi and Jang (1992) investigated mixed convective flow in a bottom heated square lid-driven cavity. The authors studied the effect of Prandtl number on the flow and heat transfer process. They found that the effects of buoyancy are more pronounced for higher values of Prandtl number, and also derived a correlation for the average Nusselt number in terms of the Prandtl number, Reynolds number and Richardson number. Prasad and Koseff (1996) experimentally investigated mixed convection heat transfer in deep lid-driven cavities heated from below. The authors observed that the heat transfer was rather insensitive to the Richardson number. Aydin (1999) studied numerically and revealed the mechanisms of aiding and opposing mixed convection in a shear- and buoyancy- driven cavity. The phenomenon inside square cavity was analyzed with moving vertical hot wall, either upwards or downwards while keeping the opposite cold wall fixed. In their work, a parametric study was carried out by varying Gr/Re^2 from 0.01 to 100 with $Pr = 0.71$ and three kinds of heat transfer regimes were identified. Further it was pointed out that the range of Gr/Re^2 for opposing mixed convection was wider than that of aiding buoyancy case. Later on, Aydin and Yang (2000) numerically studied mixed convection heat transfer in a two-dimensional square cavity having an aspect ratio of 1. In their configuration the isothermal sidewalls of the cavity were moving downwards with uniform velocity while the top wall was adiabatic. A symmetrical isothermal heat source was placed at the other adiabatic bottom wall. Mixed convection heat transfer in a two-dimensional rectangular cavity with constant heat flux from partially heated bottom wall while the isothermal sidewalls are moving in the vertical direction was numerically studied by Gau and Sharif (2004). In their work the authors considered several values of heat source length, the aspect ratio of the cavity, as well as symmetric and asymmetric placement of the heat source. The authors found that for asymmetric placement of heat source, the maximum temperature decreases and the average Nusselt number increases as the heat source is moved more and more towards the sidewall. Oztop and Dagtekin (2004) investigated numerically steady state two-dimensional mixed convection problem in a vertical two-sided lid-driven differentially heated square cavity. Hossain and Gorla (2006) investigated the effects of viscous dissipation on unsteady combined convective heat transfer to water near its density maximum in a rectangular cavity with isothermal wall. Luo and Yang (2007) numerically investigated two-dimensional flow in a two-sided lid-driven cavity containing a temperature gradient.

Analysis of the cavity phenomena incorporating a solid material extends its usability in the engineering fields. Considering the complexity of phenomenon in side an obstructed cavity with moving wall, a brief review on the relevant literature has been hereby presented. Roychowdhury et al. (2002) analyzed the natural convective flow and heat transfer features for a heated cylinder kept in a square enclosure with different thermal boundary conditions. Dong and Li (2004) studied conjugate of natural convection and conduction in a complicated enclosure. The authors investigated the influences of material character, geometrical shape and Rayleigh number on the heat transfer in overall concerned region and concluded that the flow and heat transfer increase with the increase of thermal conductivity in the solid region; both geometric shape and Rayleigh number affect the overall flow and heat transfer greatly. Braga and Lemos (2005) numerically studied steady laminar natural convection within a square cavity filled with a fixed amount of conducting solid material consisting of either circular or square obstacles. The authors showed that the average Nusselt number for cylindrical rods is slightly lower than those for square rods. Lee and Ha (2005) investigated natural convection in a horizontal layer of fluid with a conducting body in the interior, using an accurate and efficient Chebyshev spectral collocation approach. Later on, the same authors Lee and Ha (2006) also studied natural convection in horizontal layer of fluid with heat generating conducting body in the interior. Kumar and Dalal (2006) studied natural convection around a tilled heated square cylinder kept in an enclosure in the range of $10^3 \leq Ra \leq 10^6$. The authors reported detailed flow and heat transfer features for two different thermal boundary conditions and found that the uniform wall temperature heating is quantitatively different from the uniform wall heat flux heating.

A combined free and forced convection flow of an electrically conducting fluid in cavities in the presence of a magnetic field is of special technical significance because of its frequent occurrence in many industrial applications such as geothermal reservoirs, cooling of nuclear reactors, thermal insulations and petroleum reservoirs. These types of problems also arise in electronic packages, micro electronic devices during their operations. Garandet et al. (1992) studied natural convection heat transfer in a rectangular enclosure with a transverse magnetic field. Rudraiah et al. (1995a) investigated the effect of surface tension on buoyancy driven flow of an electrically conducting fluid in a rectangular cavity in the presence of a vertical transverse magnetic field to see how this force damps hydrodynamic movements. At the same time, Rudraiah et al. (1995b) also studied the effect of a magnetic field on free convection in a rectangular enclosure. The problem of unsteady laminar combined forced and free convection flow and heat transfer of an electrically conducting and heat generating or absorbing fluid in a vertical lid-driven cavity in the presence

of a magnetic field was formulated by Chamkha (2002). Very recently Rahman et al. (2009a) studied MHD mixed convection around a heat conducting horizontal circular cylinder placed at the center of a rectangular cavity along with joule heating.

1.2 Objectives of the Present Study

The objective of the present study is to analyze the effect of a heat conducting horizontal circular cylinder on MHD mixed convection in a lid-driven cavity along with joule heating using finite element technique. Above literature review clearly shows that researchers are not investigated the effect of a heat conducting horizontal circular cylinder on MHD mixed convection in a lid-driven cavity along with joule heating. In the present works the cylinder is assumed to be heat conducting keeping in view their applications in many practical situations.

2. ANALYSIS

The physical model and co-ordinate system considered in this study is given in Figure 1. It is a two-dimensional square lid-driven cavity of length L with a heat conducting horizontal circular cylinder of diameter d, placed somewhere (l_x, l_y) within the cavity. The left wall of the cavity is allowed to move upward in its own plane at a constant velocity U_0. Horizontal walls of the cavity are insulated while the left and right vertical walls are isothermal but the temperature of the right wall is higher than that of the left wall. The fluid permeated by a uniform external magnetic field B_0. The resulting convective flow is governed by the combined mechanism of driven (share and buoyancy) force and the electromagnetic retarding force.

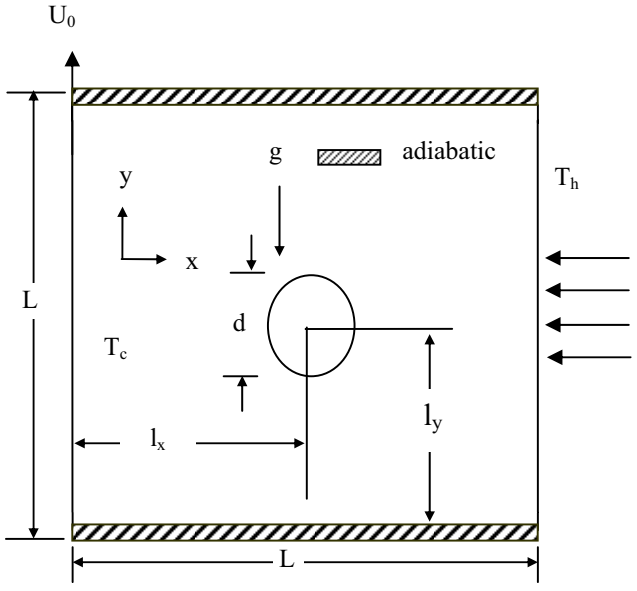

Figure 1 Schematic of the problem with the domain and boundary conditions

The magnetic Reynolds number is assumed to be small so that the induced magnetic field produced by the motion of the electrically conducting fluid is negligible compared to the applied magnetic field B_0. The density variation considered only in the body force term according to the Boussinesq approximation. Further, joule heating is considered, but pressure work, radiation and viscous dissipation are assumed to be negligible. All solid boundaries are assumed to be rigid no-slip walls. Emphasis of the effect of the cylinder configuration on the thermal phenomenon is considered.

2.1 Governing Equations

The system is considered to be two-dimensional laminar, incompressible and steady state. Moreover, the electrically conducting fluids are assumed to be Newtonian fluids with constant fluid properties except for the density in the buoyancy force term (i. e. Boussinesq approximation). In magneto fluid mechanics, fluid motion is governed by the conservation equations of mass, momentum and energy. The equation of continuity and u-momentum equation remain unchanged, but the equation of v-momentum is modified from Maxwell's field equation and Ohm's law. On the other hand, the equation of energy is modified due to joule heating considered in the cavity. Dimensionless governing equations in *UV*-velocity form can be obtained via introducing the dimensionless variables as follows:

$$X = \frac{x}{L},\ Y = \frac{y}{L},\ U = \frac{u}{U_0},\ V = \frac{v}{U_0},\ P = \frac{p}{\rho {U_0}^2},\ D = \frac{d}{L},$$

$$L_x = \frac{l_x}{L}, L_y = \frac{l_y}{L},\ \theta = \frac{(T - T_c)}{(T_h - T_c)},\ \theta_s = \frac{(T_s - T_c)}{(T_h - T_c)}$$

Based on the dimensionless variables above the governing equations (mass, momentum and energy) can be written as

$$\frac{\partial U}{\partial X} + \frac{\partial V}{\partial Y} = 0 \tag{1}$$

$$U\frac{\partial U}{\partial X} + V\frac{\partial U}{\partial Y} = -\frac{\partial P}{\partial X} + \frac{1}{Re}\left(\frac{\partial^2 U}{\partial X^2} + \frac{\partial^2 U}{\partial Y^2}\right) \tag{2}$$

$$U\frac{\partial V}{\partial X} + V\frac{\partial V}{\partial Y} = -\frac{\partial P}{\partial Y} + \frac{1}{Re}\left(\frac{\partial^2 V}{\partial X^2} + \frac{\partial^2 V}{\partial Y^2}\right) + Ri\,\theta - \frac{Ha^2}{Re}V \tag{3}$$

$$U\frac{\partial \theta}{\partial X} + V\frac{\partial \theta}{\partial Y} = \frac{1}{Re\,Pr}\left(\frac{\partial^2 \theta}{\partial X^2} + \frac{\partial^2 \theta}{\partial Y^2}\right) + J\,V^2 \tag{4}$$

For the solid cylinder

$$0 = \frac{K}{Re\,Pr}\left(\frac{\partial^2 \theta_s}{\partial X^2} + \frac{\partial^2 \theta_s}{\partial Y^2}\right) \tag{5}$$

The non-dimensional parameters that appear in the formulation are the Reynolds number ($Re = U_0 L/\upsilon$), the Grashof number ($Gr = g\beta\Delta T L^3/\upsilon^2$), square of the Hartmann number ($Ha^2 = \sigma B_0^2 L^2/\mu$), the Joule heating

parameter ($J = \sigma B_0^2 L U_0 / \rho C_p \Delta T$), the Prandtl number ($Pr = \nu/\alpha$), the Richardson number ($Ri = Gr/Re^2$) and solid fluid thermal conductivity ratio ($K = k_s/k_f$) respectively. For the present work, air is considered as the fluid medium and the Prandtl number is constant (*Pr* = 0.71). Therefore, attention is focused on the effect of cylinder size, locations and solid fluid thermal conductivity ratio on the flow and thermal fields as well as heat transfer of the system at different values of *Ri*.

2.2 Boundary Conditions

The dimensionless form of the boundary conditions can be written as

At the left wall: $U = 0, V = 1, \theta = 0$

At the right vertical wall: $U = 0, V = 0, \theta = 1$

At the solid surface: $U = 0, \ V = 0$

At the top and bottom walls: $U = 0, V = 0, \dfrac{\partial \theta}{\partial N} = 0$

At the fluid-solid interface: $\left(\dfrac{\partial \theta}{\partial N}\right)_{fluid} = K\left(\dfrac{\partial \theta_s}{\partial N}\right)_{solid}$

Where *N* is the non-dimensional distances either along *X* or *Y* direction acting normal to the surface.

The average Nusselt number at the heated wall of the cavity based on the dimensionless quantities may be expressed by $Nu = -\int_0^1 \dfrac{\partial \theta}{\partial X} dY$ and the average temperature of the fluid in the cavity is defined by $\theta_{av} = \int \theta \, d\overline{V} / \overline{V}$, where $\overline{V}$ is the cavity volume.

The non-dimensional stream function is defined as

$$U = \frac{\partial \psi}{\partial Y}, V = -\frac{\partial \psi}{\partial X}$$

2.3 Numerical Method

The methodology proposed for analyzing mixed convection in an obstructed vented cavity in our previous paper Rahman et al. (2009b) is employed here to investigate the mixed convection in an obstructed lid-driven cavity with slight modification. In order to ensure the grid-independence solutions, a series of calculation were conducted for different grid distributions. The details of grid independence test are available in Rahman et al. (2009a).

To check the adequacy of the numerical scheme, results for a two-dimensional lid driven square cavity filled with an electrically conducting fluid that generates or absorbs heat at a rate. The left wall is moving upward with a velocity and maintained at cooled condition. The right wall is hooted whereas the two horizontal walls are under adiabatic condition, which was done by Chamkha (2002). We compared the present results with their study using average Nusselt numbers for different values of Hartmann number and Grashof numbers. A good agreement was found between the present predicted results and those of Chamkha (2002) as listed in Rahman et al. (2009a).

3. RESULTS AND DISSCUSSION

The mixed convection phenomenon inside a differentially heated obstructed lid-driven cavity with the presence of a joule heating, magnetic field is influenced by the Reynolds number *Re*, Richardson number *Ri*, Prandtl number *Pr*, Hartmann number *Ha*, Joule heating parameter *J*, solid fluid thermal conductivity ratio *K*, various size and locations of the cylinder in the cavity. In order to focus on the effect of the cylinder size, locations and solid fluid thermal conductivity ratio at the three convective regimes in the cavity, we assign *Ha* = 10.0, *J* = 1.0, *Re* = 100 and *Pr* = 0.71. Moreover, the effect of cavity aspect ratio and Hartmann number on the flow and heat transfer characteristics have already been reported by Rahman et al. (2009a). The results are presented in terms of streamline and isotherm patterns at the three different regimes of flow, viz., pure forced convection, mixed convection and dominating natural convection with *Ri* = 0.0, 1.0 and 5.0 respectively. The variations of the average Nusselt number at the heated surface and average fluid temperature in the cavity are plotted for the different values of the parameters. Moreover, the variations of the average Nusselt number at the heated surface is also highlighted in tabular form.

3.1 Effect of Cylinder Size

The effect of cylinder size on the flow fields as streamlines in the cavity operating at three different values of Ri, while the values of *K* = 5.0 and $L_x = L_y = 0.5$ are keeping fixed is presented in the Figure 2. As well known from the literature, the values of the Richardson number is a measure of the importance of natural convection to forced convection. Figure 2 shows that the forced convection plays a dominant role and the recirculation flow is mostly generated only by the moving lids at low *Ri* (*Ri* = 0.0) and *D* (*D* = 0.0). The recirculation flow rotates in the clockwise direction, which is expected since the lid is moving upwards. Further at low *Ri* (*Ri* = 0.0) and the higher values of *D* (*D* = 0.2, 0.4 and 0.6), the flow patterns inside the cavity remain unchanged except the shape and position of the core of the circulatory flow. Next at *Ri* = 1.0, the natural convection effect is comparable with the forced convection effect, a pair of counter rotating rolls appear in the flow domain for the lower values of *D* (*D* = 0.0, 0.2 and 0.4), whereas the fluid flow is characterized by a clockwise rotating vortex generated by the movement of the left wall and two minor counter clockwise vortices generated by the buoyant force at the highest value of *D* (*D* = 0.6). This behavior is very logical because the large cylinder reduces the available space for the buoyancy-induced recirculation.

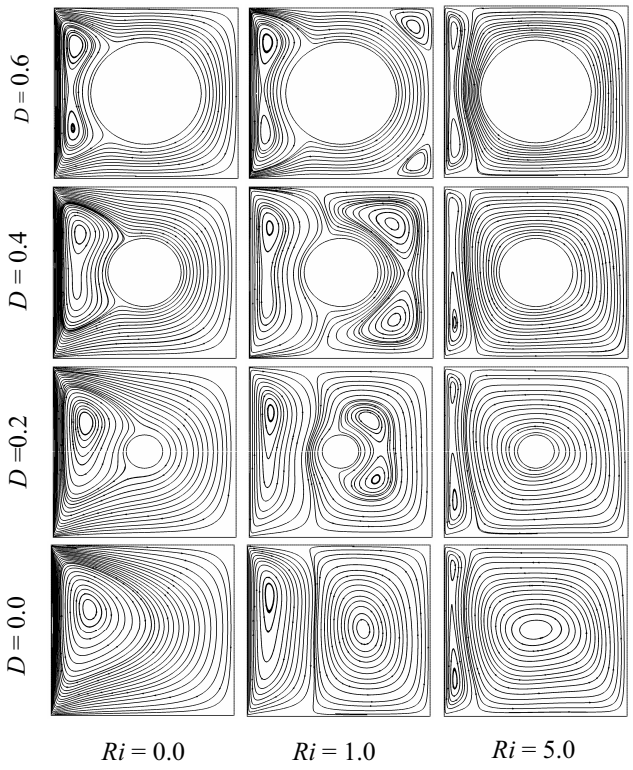

Figure 2 Streamlines for different values of D and Ri, while $K = 5.0$ and $L_x = L_y = 0.5$.

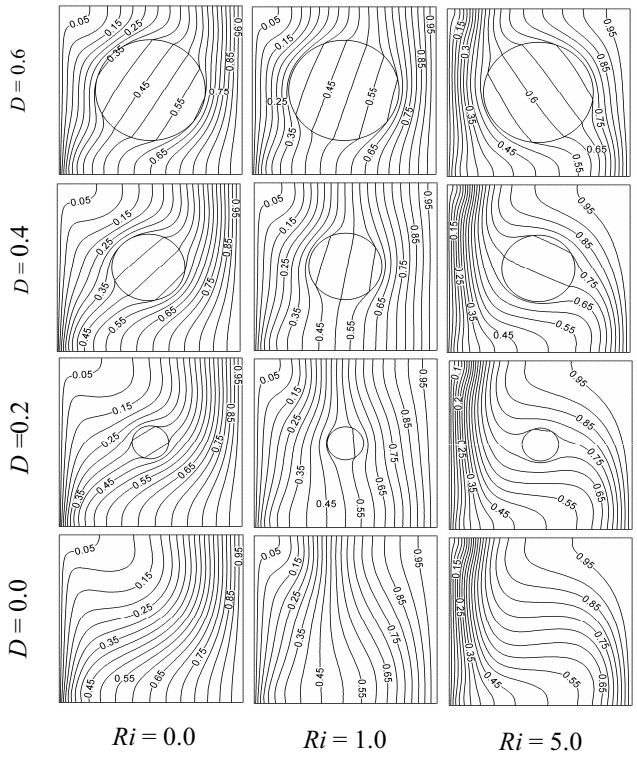

Figure 3 Isotherms for different values of D and Ri, while $K = 5.0$ and $L_x = L_y = 0.5$.

Further at $Ri = 5.0$, which is a buoyancy dominated regime, the counter clockwise rotating roll due to buoyancy force grows rapidly as a result the clockwise rotating roll due to shear driven flow becomes weaker and smaller at the four different values of D (D = 0.0, 0.2, 0.4 and 0.6) considered.The corresponding effect of the cylinder diameter on thermal fields as isotherms at various values of Ri is shown in the Figure 3. From this figure, we can ascertain that for $Ri = 0.0$ and $D = 0.0$, the isothermal lines near the hot wall are parallel to the heated surface and parabolic shape isotherms are seen at the left top corner in the cavity, which is similar to forced convection and conduction like distribution. Making a comparison of the isothermal lines for the higher values of D (D = 0.2, 0.4 and 0.6) with those for the case of without cylinder ($D = 0.0$) at $Ri = 0.0$, a slight difference is found at the left top corner in the cavity. Further for $Ri = 1.0$ and the case of without cylinder ($D = 0.0$), the isothermal lines are nearly parallel to the vertical walls in the cavity and parabolic shape isotherms at the left top corner in the cavity becomes negligible. Furthermore, similar trend is observed in the isotherms for the other values of D at $Ri = 1.0$, which is due to the conjugate effect of conduction and mixed convection flow in the cavity.

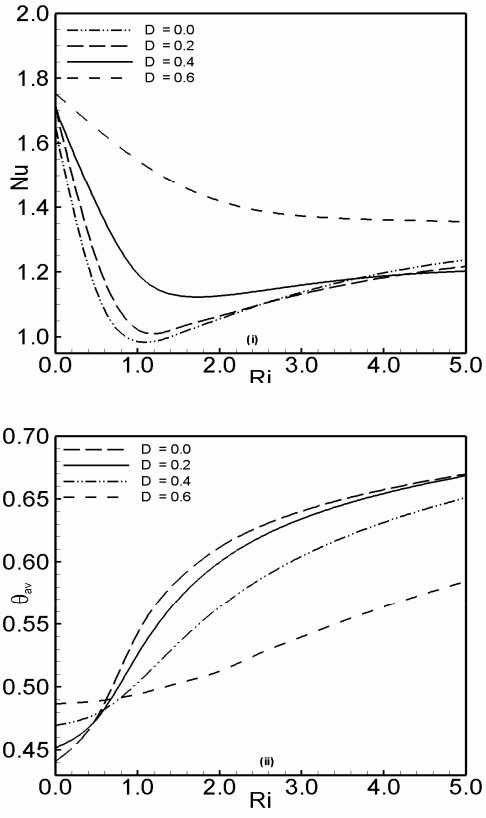

Figure 4 Effect of cylinder diameter on (i) average Nusselt number and (ii) average fluid temperature in the cavity.

As *Ri* increases further from 1.0 to 5.0, the isothermal lines near the cold wall are almost parallel to the vertical walls and parabolic shape isotherms are developed at the right top corner in the cavity, which is owing to the strong influence of the convective current in the cavity. In addition, the convective distortion in the isothermal lines near the right top corner in the cavity gradually decreases with increasing the values of *D*. This is because the larger cylinder reduces the buoyancy force effects. The variation of the average Nusselt number *Nu* at the heated surface, average temperature θ_{av} of the fluid in the cavity against *Ri* at various values of *D* is shown in the Figure 4. From this figure it is observed that in the pure forced convection (*Ri* = 0.0) the values of *Nu* is the top for the highest value of *D*, but the values of *Nu* decreases slightly with increasing *Ri* for the highest value of *D*. Moreover, the values of *Nu* decreases very quickly in the forced convection dominated region and increases gradually in the free convection dominated region at the lower values of *D* (*D* = 0.0, 0.2 and 0.4). On the other hand, maximum average Nusselt number is always found at the highest *D*. This is also supported from the obtained actual numerical values of *Nu* as shown in the Table 1. However, average temperature θ_{av} of the fluid in the cavity increases slightly at the highest *D* (*D* = 0.6) and rapidly at lower values of *D* (*D* = 0.0, 0.2 and 0.4) with increasing *Ri*.

3.2 Effect of solid fluid thermal conductivity ratio

The flow fields in terms of computed streamlines for the four representative values of the solid fluid thermal conductivity ratio *K* (*K* = 0.2, 1.0, 5.0 and 10.0), while *D* = 0.2, $L_x = L_y$ = 0.5 is shown in Figure 5.

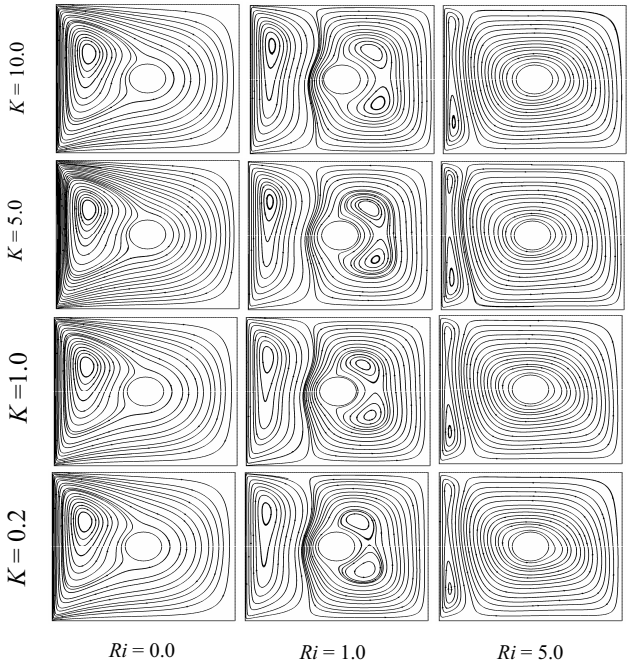

Figure 5 Streamlines for different values of *K* and *Ri*, while *D* = 0.2 and $L_x = L_y$ = 0.5.

For *Ri* = 0.0 and *K* = 0.2, it is be seen from the Figure 5 that a unicellular clockwise vortex is developed in the cavity, due to the only shear force induced by the left moving wall. However, the streamlines for the four values of *K* at *Ri* = 0.0 appear to be almost identical. This behavior is rational because thermal conductivity of the solid has negligible effect in flow field. Now for *Ri* = 1.0 and *K* = 0.2, it can be seen from the figure 5 that a pair of counter rotating vortices are formed in the flow domain, of which the clockwise vortex near the left wall is small in size than the counter clockwise vortex near the right wall. It is also observed that the counter clockwise vortex is two-cellular. In addition, visual examination of the streamlines does not reveal any significant difference among the different values of *K* at *Ri* = 1.0, owing to the same reason as stated beforehand. Further at *Ri* = 5.0 and different values of *K*, it is clearly seen that the counter clockwise vortex spreads and thereby squeezes the clockwise vortex, indicating a sign of supremacy of natural convection in the cavity. It is also seen that the streamline plots are independent of the thermal conductivity ratios *K*. Now from the Figure 6 it is reminder that the thermal conductivity of the inner cylinder affects strongly the isotherm structures in the cavity. At low *Ri* = 0.0 and *K* = 0.2, the isotherms near the hot wall are parallel to the vertical walls and the isothermal lines start to turn back towards the hot wall near the left top corner of the cavity, which gives a clear indication that a conduction dominated heat transfer at the vicinity of the hot wall and higher forced convection and conduction dominated heat transfer in the upper part of the cavity.

Table 1 Variation of average Nusselt number with cylinder diameter and Richardson number.

Ri	Nu			
	D = 0.0	D = 0.2	D = 0.4	D = 0.6
0.0	1.643882	1.710726	1.706358	1.753162
0.5	1.141781	1.239607	1.410516	1.645498
1.0	0.985516	1.022651	1.195203	1.547871
1.5	1.009741	1.028463	1.127099	1.471043
2.0	1.055573	1.064352	1.126294	1.419329
2.5	1.099580	1.100379	1.142134	1.389025
3.0	1.137945	1.132416	1.159809	1.373009
3.5	1.170392	1.159872	1.175287	1.365026
4.0	1.197434	1.182924	1.187559	1.360839
4.5	1.219715	1.201949	1.196579	1.357858
5.0	1.237833	1.217358	1.202627	1.354560

Making a comparison of the isothermal lines for different values of K at Ri = 0.0, no significant difference is found except the shift of the isothermal lines from the center of the inner cylinder. As Ri increases from 0.0 to 1.0, the distortion in isothermal lines become significant, as a result the isotherms become parallel to the vertical walls, indicating the comparable effect of the conduction and mixed convection mechanisms. As Ri increases further to 5.0, convective distortion of the isotherms occur throughout the cavity due to the strong influence of the convective current in the cavity. In this case it is also seen that a thermal boundary layer is developed near the cold wall for the four different values of K.

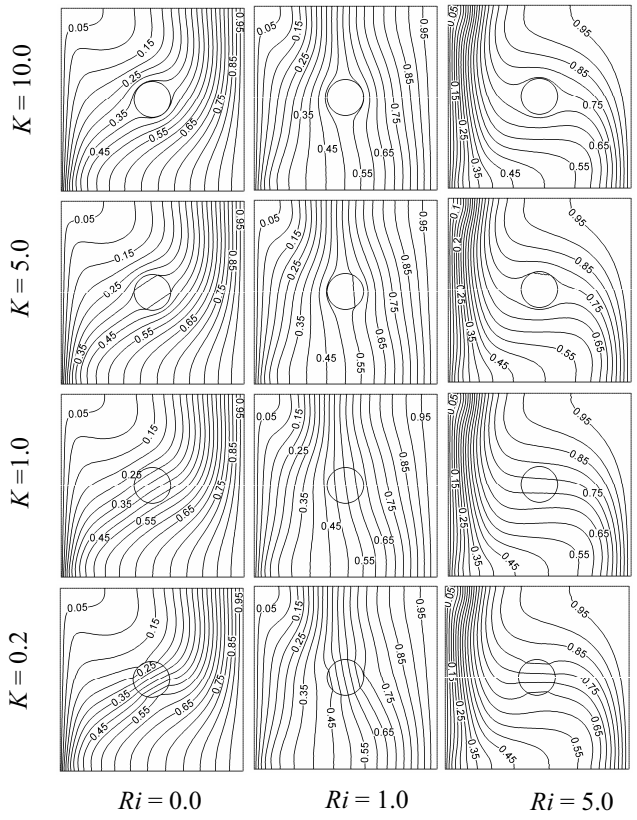

Figure 6 Isotherms for different values of K and Ri, while D = 0.2 and $L_x = L_y$ = 0.5.

Average Nusselt number Nu at the hot wall, average fluid temperature θ_{av} in the cavity is plotted as a function of Richardson number at four different values of solid fluid thermal conductivity ratio K is shown in the Figure 7. Concentrating on each plot separately for a particular values of K, the trend of the values of Nu are decreasing with increasing Ri up to 1.0 and beyond these values of Ri, the values of Nu is found to increases gradually with Ri. However, in the pure forced convection (Ri = 0.0) the value of Nu is highest for the lowest value of K, but in the forced convection dominated region it is the top for the highest values of K and beyond these values of Ri, the average Nusselt number Nu is also the peak at the lowest value of K, which are documented in the Table 2. Finally, from this figure, it is also observed that the average temperature θ_{av} of the fluid in the cavity increases monotonically with Ri.

3.3 Effect of cylinder location

The dependence of flow fields on the locations of the inner cylinder can be observed in the plots of streamlines at various values of the Richardson number Ri is shown in the Figure 8, while D = 0.2 and K = 5.0. From the left column of this figure, it is seen that in the pure forced convection region (Ri = 0.0) the flow patterns inside the cavity remain unchanged at the different locations of the cylinder, except the shape of the core of the circulatory flow. As Ri increases to 1.0, the effect of buoyant force and the shear force are of the same order of magnitude, a shear cell is formed adjacent to the moving wall and a vortex cell caused due to buoyant force is seen near the hot wall at different locations of the cylinder. However, in the mixed convection region it is also seen that, when the inner cylinder moves closer to the left cold wall along the mid-horizontal plane, the shear driven vortex becomes two cellular and buoyancy induced vortex becomes uni-cellular.

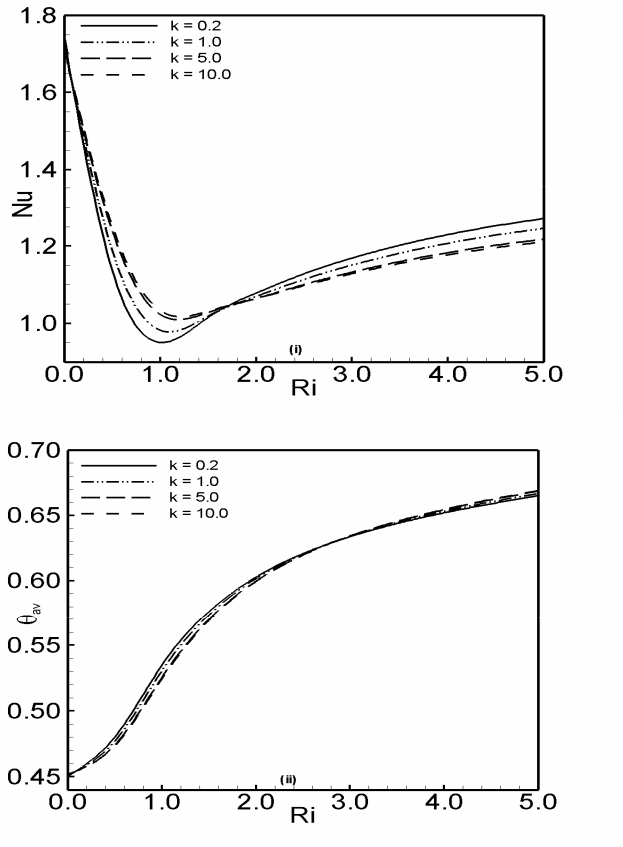

Figure 7 Effect of solid fluid thermal conductivity ratio on (i) average Nusselt number and (ii) average fluid temperature in the cavity.

If the cylinder moves further closer to the heat source along the mid-horizontal plane an opposite result is observed as compared to the previous position. Furthermore when the cylinder moves near the bottom and top insulated wall of the cavity along the mid vertical plane, then two uni-cellular counter rotating vortices are formed in the cavity. It is also seen that the size of the vortices are almost identical. Finally, when the Richardson number *Ri* increases to 5.0, the strength of the velocity circulating in the cavity increases, the size of the buoyancy induced vortex becomes larger than the share induced vortex at all values of the cylinder locations considered, because of the stronger convection effects of the increased Richardson number. The dependence of the thermal fields on locations of the inner cylinder in the cavity can be obtained in the plots of the isotherms at various values of the cylinder locations and Richardson number *Ri* is shown in Figure 9, while $D = 0.2$ and $K = 5.0$.

Table 2 Variation of average Nusselt number with solid fluid thermal conductivity ratio and Richardson number.

Ri	*Nu*			
	$K = 0.2$	$K = 1.0$	$K = 5.0$	$K = 10.0$
0.0	1.735829	1.722377	1.710726	1.708439
0.5	1.136467	1.187800	1.239607	1.251436
1.0	0.950693	0.981962	1.022651	1.033299
1.5	1.015338	1.018857	1.028463	1.031755
2.0	1.078242	1.069832	1.064352	1.063740
2.5	1.128226	1.113792	1.100379	1.097649
3.0	1.168726	1.150669	1.132416	1.128377
3.5	1.202060	1.181486	1.159872	1.154919
4.0	1.229628	1.207111	1.182924	1.177271
4.5	1.252361	1.228240	1.201949	1.195726
5.0	1.270942	1.245442	1.217358	1.210650

At $Ri = 0.0$ and different locations of the inner cylinder, the isothermal lines near the heat source are parallel to the right vertical wall and become skewed near the left top corner of the cavity, due to the dominating influence of the conduction and forced convection heat transfer. Further increase of *Ri* to 1.0, the isothermal lines become almost parallel to the vertical walls for all the locations of the cylinder owing to the conjugate effect of conduction and mixed convection. Lastly, at $Ri = 5.0$, convective distortion of the isothermal lines occurred throughout the cavity due to the strong influence of the convective current and a thermal boundary layer is developed near the cold wall at all values of the cylinder locations considered.

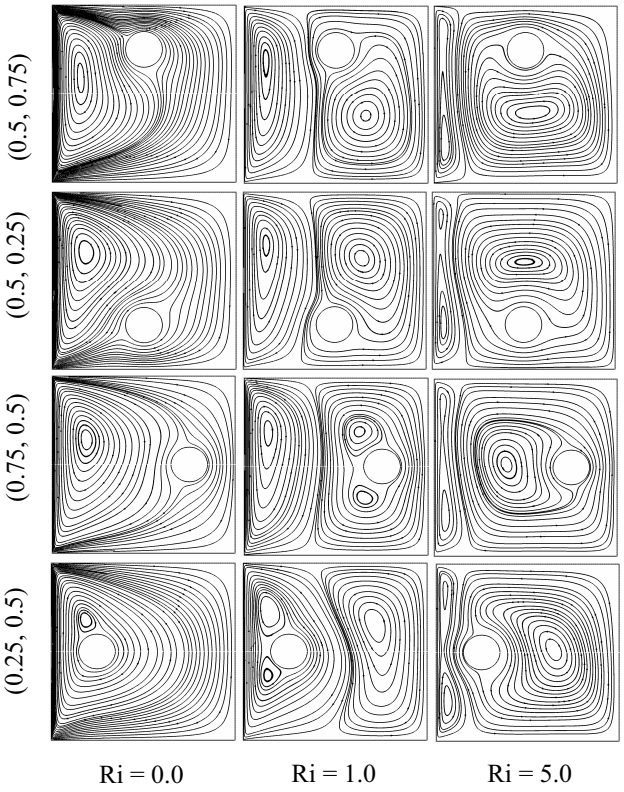

Figure 8 Streamlines for different values of (L_x, L_y) and Ri, while $D = 0.2$ and $K = 5.0$.

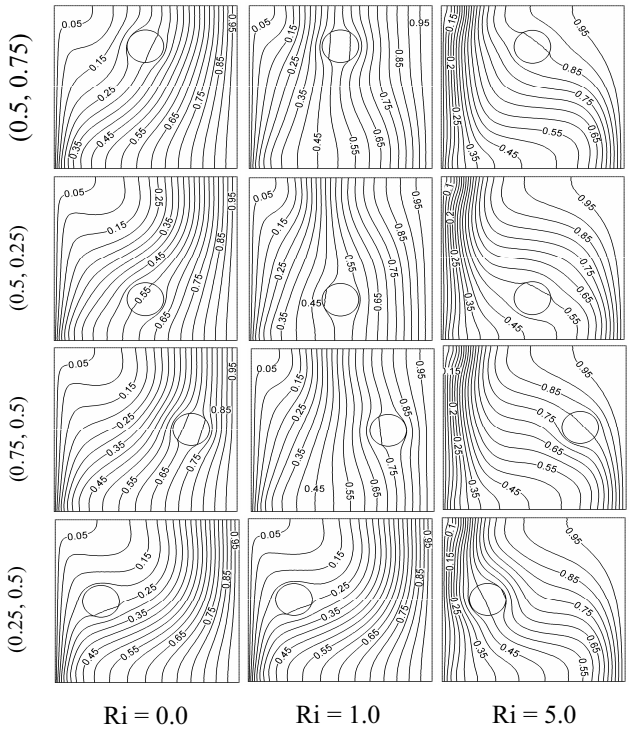

Figure 9 Isotherms for different values of (L_x, L_y) and *Ri*, while $D = 0.2$ and $K = 5.0$.

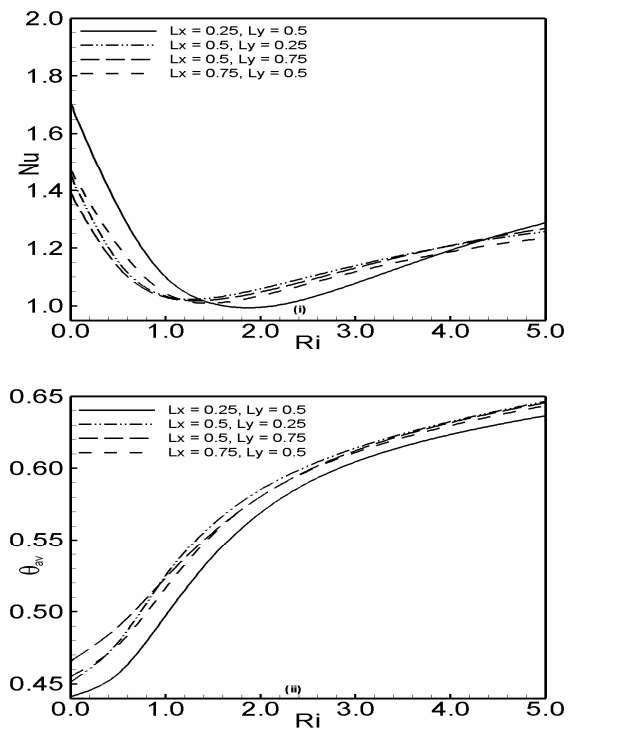

Figure 10: Effect of cylinder locations on (i) average Nusselt number and (ii) average fluid temperature in the cavity.

Table 3 Variation of average Nusselt number with cylinder locations and Richardson number

Ri	*Nu*			
	(0.25, 0.5)	(0.5, 0.25)	(0.5, 0.75)	(0.75, 0.5)
0.0	1.702954	1.449321	1.389233	1.468700
0.5	1.342464	1.154362	1.134795	1.208068
1.0	1.100091	1.033496	1.030037	1.044595
1.5	1.008073	1.028374	1.020831	1.009662
2.0	0.995173	1.059638	1.048289	1.035423
2.5	1.026419	1.099846	1.088562	1.076644
3.0	1.078620	1.139807	1.131534	1.118232
3.5	1.136758	1.176249	1.172479	1.155607
4.0	1.192977	1.208107	1.209340	1.187580
4.5	1.243755	1.235211	1.241419	1.214121
5.0	1.287813	1.257767	1.268685	1.235600

The average Nusselt number *Nu* at the heated surface and average fluid temperature θ_{av} in the cavity is plotted against Richardson numbers in Figure 10 for the four different locations of the inner cylinder. For each locations of the cylinder, the *Nu*-*Ri* profile is parabolic shape shows two distinct zones depending on Richardson number. Up to a certain value of *Ri* the distribution of *Nu* smoothly decreases with increasing *Ri* and beyond these values of *Ri* it is increases with *Ri*. Furthermore, the values of *Nu* are found maximum, when the inner cylinder moves closer to the left wall along the mid-horizontal plane at the values of $Ri < 1.5$, and beyond these values of *Ri* it is the highest when the cylinder moves near the bottom insulated wall of the cavity along the mid vertical plane. This is also supported from the numerical values obtained for the case shown in the Table 3. On the other hand, average fluid temperature θ_{av} in the cavity increases monotonically with *Ri* at each locations of the cylinder. Besides, the value of θ_{av} is always lower, when the cylinder center is at (0.25, 0.5).

4. CONCLUSION

In these analyses, the effect of a heat conducting horizontal circular cylinder on MHD mixed convection in a lid-driven cavity along with joule heating were presented using the parameters as solid fluid thermal conductivity ratio *K*, various size and locations of the cylinder in the cavity. A detailed analysis for the distribution of streamlines, isotherms, average Nusselt number at the hot wall and average fluid temperature in the cavity were carried out to investigate the effect of the dimensionless parameters. In view of the obtained results, following findings were summarized:

- Cylinder size *D* has significant effect on the flow and thermal fields in the cavity. Higher average Nusselt number was always found for the largest value of *D*. The average temperature θ_{av} of the fluid in the cavity was lesser for $D = 0.0$ in the forced convection dominated region, but for $D = 0.6$ in the free convection dominated region.

- Thermal conductivity ratio of the solid to that of the fluid, K affects the isotherm distribution in the inner body, thus it affects also isotherms in the entire cavity, whereas the distribution of streamlines are independent on the thermal conductivity ratio K. The effect of K on the average Nusselt number Nu depends upon the cylinder size. Relatively large effect on thermal phenomenon was observed for a big size cylinder (not shown). A deficiency in the heat transfer rate is obtained when the cylinder size is decreased. A similar trend is also observed on the average temperature of the fluid in the cavity.

- The location of the inner cylinder was one of the most important parameter on fluid flow and temperature fields as well as heat transfer characteristics. Moreover, noticeably different flow behaviors and heat transfer

characteristics were observed among the three different flow regimes. The value of the average Nusselt number was greater if the solid cylinder was placed near the cold wall along the mid-horizontal plane at $Ri < 1.5$ and beyond these values of Ri it is the highest when the cylinder moves near the bottom insulated wall of the cavity along the mid vertical plane. On the other hand, the average fluid temperature was always lesser when the solid cylinder was placed near the cold wall along the mid-horizontal plane.

REFERENCE

Aydin, O., 1999. Aiding and opposing mechanisms of mixed convection in a shear- buoyancy driven cavity, Int. Commun. Heat Mass Transfer, Vol. 26, pp. 1019-1028.

Aydin, O., Yang, W. J., 2000. Mixed convection in cavities with a locally heated lower wall and moving sidewalls, Numer. Heat Transfer, Part A, Vol. 37, pp. 695-710.

Braga, E. J., de Lemos, M. J. S., 2005. Laminar natural convection in cavities filed with circular and square rods, Int. Commun. in Heat and Mass Transfer, Vol. 32, pp. 1289-1297.

Chamkha, A. J., 2002. Hydromagnetic combined convection flow in a vertical lid-driven cavity with internal heat generation or absorption, Numer. Heat Transfer, Part A, Vol. 41, pp. 529-546.

Dong, S. F., Li, Y.T., 2004. Conjugate of natural convection and conduction in a complicated enclosure, Int. J. of Heat and Mass Transfer, Vol. 47, pp. 2233-2239.

Garandet, J. P., Alboussiere, T., Moreau, R., 1992. Buoyancy driven convection in a rectangular enclosure with a transverse magnetic field, Int. J. of Heat Mass Transfer, Vol. 35, pp. 741-748.

Guo, G., Sharif, M. A. R., 2004. Mixed convection in rectangular cavities at various aspect ratios with moving isothermal sidewalls and constant flux heat source on the bottom wall, Int. J. of Thermal Sciences, Vol. 43, pp. 465-475.

Hossain, M. A., Gorla, R. S. R., 2006. Effect of viscous dissipation on mixed convection flow of water near its density maximum in a rectangular enclosure with isothermal wall, Int. J. of Numer. Methods for Heat and Fluid Flow, Vol. 16, No. 1, pp. 5-17.

Jaluria, Y., Torrance, K. E., 1986. Computational Heat Transfer. Hemisphere, Washington.

Kumar De, A., Dalal, A., 2006. A numerical study of natural convection around a square, horizontal, heated cylinder placed in an enclosure, Int. J. of Heat and Mass Transfer, Vol. 49, pp. 4608-4623.

Lee, J. R., Ha, M. Y., 2005. A numerical study of natural convection in a horizontal enclosure with a conducting body, Int. J. of Heat and Mass Transfer, Vol. 48, pp. 3308-3318.

Lee, J. R., Ha, M. Y., 2006. Numerical simulation of natural convection in a horizontal enclosure with a heat-generating conducting body, Int. J. of Heat and Mass Transfer, Vol. 49, pp. 2684-2702.

Luo, W. J., Yang, R. J., 2007. Multiple fluid flow and heat transfer solutions in a two-sided lid-driven cavity, Int. J. of Heat and Mass Transfer, Vol. 50, pp. 2394-2405.

Moallemi, M. K., Jang, K. S., 1992. Prandtl number effects on laminar mixed convection heat transfer in a lid-driven cavity, Int. J. Heat and Mass Transfer, Vol. 35, pp. 1881-1892.

Oztop, H. F., Dagtekin, I., 2004. Mixed convection in two-sided lid-driven differentially heated square cavity, Int. J. of Heat and Mass Transfer, Vol. 47, pp. 1761-1769.

Prasad, A. K., Koseff, J. R., 1996. Combined forced and natural convection heat transfer in a deep lid-driven cavity flow, Int. J. Heat and Fluid Flow, Vol. 17, pp. 460-467.

Rahman, M. M., Alim, M. A. Mamun, M. A. H., 2009b. Finite Element Analysis of Mixed Convection in a Rectangular Cavity with a Heat-Conducting Horizontal Circular Cylinder, Nonlinear Analysis: Modelling and Control, Vol.14, No.2, pp. 217-247.

Rahman, M. M., Alim, M. A., Chowdhury, M. K., 2009a. Magneto hydrodynamics mixed convection around a heat conducting horizontal circular cylinder in a rectangular lid-driven cavity with joule heating, J. of Sci. Res., Vol. 1, No. 3, pp. 461-472.

Roychowdhury, D.G, Das, S.K., Sundararajan, T.S., 2002. Numerical simulation of natural convection heat transfer and fluid flow around a heated cylinder inside an enclosure, Heat and Mass Transfer, Vol. 38, pp. 565-576.

Rudraiah, N., Barron, R. M., Venkatachalappa, M., Subbaraya, C. K., 1995b. Effect of magnetic field on free convection in a rectangular enclosure, Int. J. Engng. Sci., Vol. 33, pp. 1075-1084.

Rudraiah, N., Venkatachalappa, M., Subbaraya, C. K., 1995a. Combined surface tension and buoyancy-driven convection in a rectangular open cavity in the presence of magnetic field, Int. J. Non-linear Mech., Vol. 30, No. 5, pp. 759-770.